REPORT DOCUMENTATION PAGE

Form Approved
OMB No. 0704-0188

1. AGENCY USE ONLY (Leave blank)	2. REPORT DATE	3. REPORT TYPE AND DATES COVERED
		Reprint (1993)

4. TITLE AND SUBTITLE
Ultrashort High Peak Power Lasers and Generation of Hard Incoherent X-Rays

5. FUNDING NUMBERS
ARO MIPR 130-94

6. AUTHOR(S)
C. P. J. Barty, G. L. Gordon III, J. D. Kmetec, B. E. Lemoff, and S. E. Harris

7. PERFORMING ORGANIZATION NAME(S) AND ADDRESS(ES)
Edward L. Ginzton Laboratory
Stanford University
Stanford, CA 94305

8. PERFORMING ORGANIZATION REPORT NUMBER

9. SPONSORING/MONITORING AGENCY NAME(S) AND ADDRESS(ES)
U.S. Army Research Office
P. O. Box 12211
Research Triangle Park, NC 27709-2211

10. SPONSORING/MONITORING AGENCY REPORT NUMBER
ARO 28978.12-PH

11. SUPPLEMENTARY NOTES
The view, opinions and/or findings contained in this report are those of the author(s) and should not be construed as an official Department of the Army position, policy, or decision, unless so designated by other documentation.

12a. DISTRIBUTION/AVAILABILITY STATEMENT
Approved for public release; distribution unlimited.

12b. DISTRIBUTION CODE

13. ABSTRACT *(Maximum 200 words)*

The design, construction, and use of high peak power infrared laser pulses for the generation of diagnostic (20 keV to 150 keV) x-rays are discussed. A review of recent laser-plasma generation of diagnostic x-rays is presented. The advantages of such sources include subpicosecond pulse duration and extremely small source size. Because of their short duration, it should be possible to form time-gated medical images with up to eight times less x-ray flux than with conventional x-ray sources. Details of a next generation laser driver are also presented. Generation of 20-fs pulses from a regeneratively initiated, self-mode-locked Ti:Sapphire laser is described. Techniques for amplification of these pulses to peak powers of 5 TW are presented.

14. SUBJECT TERMS
Ultrashort High Peak Power Lasers
Generation of Hard Incoherent X-Rays

15. NUMBER OF PAGES

16. PRICE CODE

17. SECURITY CLASSIFICATION OF REPORT	18. SECURITY CLASSIFICATION OF THIS PAGE	19. SECURITY CLASSIFICATION OF ABSTRACT	20. LIMITATION OF ABSTRACT
UNCLASSIFIED	UNCLASSIFIED	UNCLASSIFIED	UL

PROCEEDINGS

OF THE
INTERNATIONAL CONFERENCE
ON

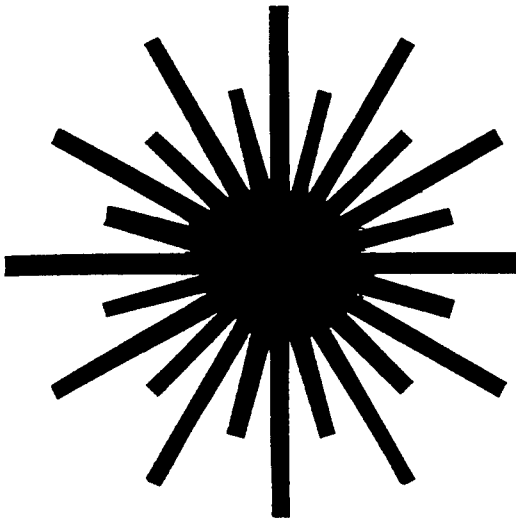

LASERS '92

HOUSTON, TEXAS **DECEMBER 7–10, 1992**

C.P. Wang
Editor

CONFERENCE SPONSORED BY
THE SOCIETY FOR OPTICAL & QUANTUM ELECTRONICS

STS PRESS • McLEAN, VA • 1993

ULTRASHORT HIGH PEAK POWER LASERS AND GENERATION OF HARD INCOHERENT X-RAYS

C. P. J. Barty, C. L. Gordon III, J. D. Kmetec, B. E. Lemoff and S. E. Harris

Edward L. Ginzton Laboratory
Stanford University
Stanford, California 94305

Abstract

The design, construction, and use of high peak power infrared laser pulses for the generation of diagnostic (20 keV to 150 keV) x-rays are discussed. A review of recent laser-plasma generation of diagnostic x-rays is presented. The advantages of such sources include subpicosecond pulse duration and extremely small source size. Because of their short duration, it should be possible to form time-gated medical images with up to eight times less x-ray flux than with conventional x-ray sources. Details of a next generation laser driver are also presented. Generation of 20-fs pulses from a regeneratively initiated, self-mode-locked Ti:sapphire laser is described. Techniques for amplification of these pulses to peak powers of 5 TW are presented.

1. Introduction

The development of Ti:sapphire as a tunable, solid state laser material has allowed the construction of reliable, high peak power, high repetition rate, ultrashort duration, infrared laser pulses. Pulses of less than 20 fs have been produced from mode-locked Ti:sapphire oscillators.[1-4] Amplification of longer duration (~ 120 fs) pulses has resulted in terawatt peak powers at pulse repetition rates of 10 Hz.[5, 6] These laser systems allow the study of laser matter interactions at intensities greater than 10^{18} W/cm^2.

In laser-produced-plasma experiments such pulses have lead to the production of hard, incoherent x-rays with energies as high as 1.5 MeV.[7] In these experiments, copious amounts of diagnostic x-rays (20 keV to 150 keV) are also generated. This fact suggests that ultrashort-pulse-pumped, laser-produced-plasma x-ray sources may be useful in medical x-ray imaging applications. In this paper, laser-produced-plasma generation of medical x-rays will be briefly reviewed. The possible advantages of such a source over conventional x-ray laser devices will be outlined. These advantages include short x-ray pulse duration and small x-ray source size. It will be shown that short pulse duration may be used to reduce patient exposure by up to eight times for a given signal-to-noise limited image.

In addition, this paper will review our efforts to construct the next generation, short pulse, high peak power laser driver for x-ray generation. In order to produce high average power sources that can compete with conventional x-ray devices, it will be necessary to produce x-rays with less laser energy. Previous laser-plasma experiments indicate that the x-ray yield is proportional to the peak electric field of the laser pulse.[8] Thus, if the laser pulse duration can be reduced, efficient generation can occur at a lower laser energy and higher repetition rate. The generation of 20-fs infrared pulses from a mode-locked Ti:sapphire laser will be discussed. Techniques for amplification of these pulses to energies > 100 mJ will also be presented.

2. Laser-Produced-Plasma, Diagnostic X-Ray Source

2.1. Summary of laser produced plasma x-ray experiments

In 1991 a 0.5 TW laser system based on amplification in Ti:sapphire was developed at Stanford.[5] The output of this system consisted of a 120-fs pulses with up to 60 mJ of energy at a repetition rate of ~ 5 Hz. Because of unsuppressed amplified spontaneous emission in the regenerative amplification stages of the system, the resulting pulses were accompanied by a low energy (~ 1 mJ) long duration (~ 5 ns) pedestal.

In laser-produced plasma experiments, 120-fs and ~ 40-mJ pulses from this system were focused with an off-axis parabolic mirror onto solid targets.[7] Focal spot sizes on the order of 3 μm and intensities on the order of 5 x 10^{18} W/cm^2 were achieved. Because of the pulse pedestal, a low-density plasma is created and expands from the target surface prior to the arrival of the high peak power, short duration, main pulse. It is believed that the short-duration pulse accelerates electrons in this preformed plasma to MeV energies. These hot electrons then collide with the solid target and, in the process, give up their energy in the form of Bremsstrahlung x-rays. This type of x-ray source has some interesting features. The duration the source will be bounded by the transit time of the electrons through the target material. For thin (~ 1 mm) targets and MeV electrons the duration should be less

than 1 ps. In addition, the source size in the longitudinal dimension is limited by the stopping distance for the given electron energy. For lower-energy (~ 100 keV) electrons, this distance will be extremely small, on the order of 10 μm.

The x-rays produced in this way were measured with calibrated NaI detectors. Crude estimates of the spectral distribution of the x-rays were determined by measuring the yield for various metal filters and by pulse height analysis. With these techniques, it was determined that the x-ray distribution could not be conveniently characterized by a single temperature. Instead, the x-rays in the 20 keV to 150 keV range were better fit by a 1/E dependence. The yield for higher energy photons fell off faster. X-rays with energies up to 1.5 MeV were observed. The yield for all x-rays was approximately proportional to Z of the target material. The highest yield was obtained with ~ 1-mm thick tantulum targets. The total yield as a function of input energy is shown in Fig. 1. The dependence is fit well by a 3/2 power law.

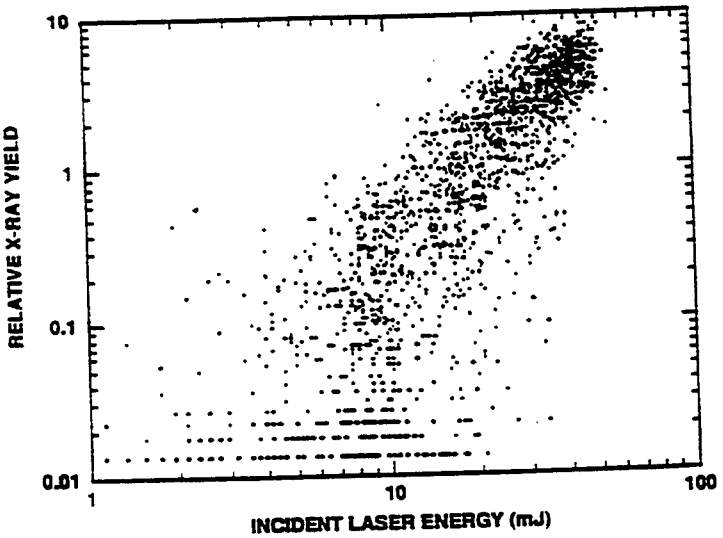

Figure 1. X-ray yield as a function of input laser energy.

2.2. Comparison of laser-produced-plasma x-ray source with conventional x-ray devices

The 3/2 power law dependence of x-ray yield suggests that the laser-driven x-ray source is similar to rotating anode x-ray tubes[9] used in medical imaging applications. In the latter device, an electron beam is accelerated trough a potential, V, and impinges upon a high-Z target. The efficiency of such a device (i.e. yield/input) is roughly 10^{-9} ZV. The efficiency of the laser-driven source is proportional to the square root of the input laser energy or intensity, which is proportional to the peak electric field of the input pulse. Thus, efficiency for both sources is proportional to the atomic number of the target material and electric field.

A comparison of the present laser-driven x-ray source and a conventional, state-of-the-art x-ray tube (Siemens Model # Meg 125/30/82C) is given in Table 1. The major deficiency of the laser-driven source is its low average power. However, it is not unreasonable to expect that future laser-driven sources may produce equivalent x-ray fluxes. As will be shown in the next section, it is possible with a short-duration (~ 1 ps) x-ray source to obtain the same quality image but with eight times less x-ray flux than

	Rotating Anode X-ray Tube	Laser-Driven X-ray Source	Future Laser-Driven Source
Shots/Second	30	5	1000
Pump Energy Deposited	2.75 J	40 mJ	8 mJ
Efficiency	1%	0.3%	1%
Average X-ray Power	825 mW	0.6 mW	100 mW
X-ray Pulse Duration	5 ms	< 1 ps	~100 fs
X-ray Source Size	1 mm x 1 mm	<250 μm x 250 μm	~10 μm x 10 μm

Table 1. Comparison of conventional and laser-driven x-ray sources.

a long duration (~ 5 ms) source. In addition, the laser system used in past studies was not optimized for x-ray production. Also included in Table 1 are the projected laser-driven source parameters for a higher repetition rate, shorter pulse, laser driver. Since x-ray yield is proportional to the peak electric field of the laser pulse, it should be possible to obtain an equivalent x-ray flux at a lower laser pulse energy if one reduces the laser pulse duration. A reduction in laser pulse duration of five is now possible and would allow efficient production of x-rays with ~ 8 mJ of laser energy. Infrared pulses of this energy may be produced at 1-kHz repetition rates.[10] Under these conditions, using the techniques described in the next section and assuming only slightly better conversion efficiency than previously measured, the effective x-ray flux of the laser-driven source would be equivalent to the conventional x-ray tube. However, the patient would receive an eight times less dosage. In addition, because of the much smaller x-ray source size, it should be possible to improve resolution by about an order of magnitude.

3. Time Gated X-Ray Imaging

In traditional x-ray imaging, three things may happen to the x-ray photons as they pass through a sample: they may be absorbed by dense material, they may undergo a scattering event, or they may pass through the sample unaffected. It is the difference in flux between the unaffected or ballistic photons and those that are absorbed that is responsible for the formation of an image at the detector. Scattered photons that also reach the detector will decrease the contrast ratio and increase the noise of the image. In mammalian samples, this can be a significant problem. Typically, for every one ballistic photon passing through 20 cm of mammalian tissue with 2 cm of bone density material in the path, there will be ~ 0.1 absorption events and ~ 7 scattering events.[11]

To illustrate this problem, let us consider the hypothetical case of a material that has only absorption and no scattering. In this case the contrast ratio, CR, of the image that is formed is

$$CR = \Delta N / N_B \qquad \text{Eq. (1)}$$

where N_B is the total number of x-ray photons incident on the sample and ΔN is the number difference of the ballistic and absorbed photons. This image will have a signal-to-noise ratio that is determined by the statistics of the x-rays. At low photon numbers, the x-rays may be modeled by a Poisson distribution. Thus, the signal-to-noise ratio, SNR, is given by

$$SNR = \Delta N / \sqrt{N_B} = CR\sqrt{N_B} \qquad \text{Eq. (2)}$$

Now if we consider the same material but add N_S scattered photons to the image then CR and SNR become

$$CR = \Delta N / (N_B + N_S) \qquad \text{Eq. (3)}$$

$$SNR = \Delta N / \sqrt{N_B + N_S} \qquad \text{Eq. (4)}$$

Clearly, CR and SNR are decreased by the presence of scattering. It is possible to increase CR and SNR in either case by increasing the x-ray flux. However, this is not practical when working with live samples. In this situation, the minimum acceptable SNR of the image determines the flux that is used.

Because the x-rays from a laser-driven source have a duration that is short (< 1 ps) with respect to the transit time through the sample (~ 1 ns), it may be possible to eliminate the effects of scattered photons by time gating. When compared with ballistic photons, scattered photons travel a longer path and thus experience a longer delay in reaching the same location at the detector. If one uses a detector that may be turned off rapidly after the arrival of the ballistic photons, then the scattered photons may be removed from the image. For the same SNR, it is then possible to construct an image with much less flux. For mammalian objects, this can be seen by setting the right-hand sides of Eqs. (2) and (4) equal and making the substitution $N_S = 7N_B$. In this case, the number of photons needed to form the image is eight times less than that needed with time-integrated detection. An eight times reduction in dosage would greatly benefit many medical procedures. For instance, in x-ray coronary angiography, a patient may receive a full year's dose in a single 30-minute session.[12]

The degree of image improvement or dose reduction will, of course, be limited by the speed with which the detector may be gated. Shorter duration gates will allow the elimination of smaller angle-scattering events. A 50-ps time gate would eliminate all scattered photons which experience a path difference of greater than 1.5 cm with respect to the ballistic path. Relatively simple microchannel plate detectors with gate times of this order have been developed for time-resolved studies of x-ray emission in inertial confinement fusion experiments.[13]

Obviously, in order for time gating to be practical, the duration of the x-ray source must be short compared to the transit time through the sample. The laser-driven source is ideal in this respect. In addition, because of its small source size, it may be possible to image much smaller objects than currently feasible. Capillaries in angiographic procedures, for example, cannot be resolved with conventional sources.[14]

4. Short Pulse Oscillator Development

4.1. Regeneratively initiated, self-mode-locking

In order to produce x-rays at a lower laser pulse energy it will be necessary to reduce the pulse duration of the laser source. The large gain bandwidth of Ti:sapphire should, in principle, support pulses of ~ 3 fs in duration. However, phase distortions in the laser oscillator limit the pulse duration that may be achieved. We have constructed a 20-fs oscillator capable of producing 500 kW peak power pulses at a repetition rate of 100 MHz.[1] In this oscillator, cavity cubic phase errors are reduced by correct design and placement of a GDD compensating prism pair. In addition, pulse duration is shown to decrease and spectral content to increase as intracavity power is increased. Control of intracavity focusing and a high-modulation-depth, acousto-optic modulator allow the intracavity power to be maximized.

In this oscillator, the intracavity focusing mirrors, 2 cm Ti:sapphire rod, and rod housing are taken from a commercial cw Ti:sapphire laser (Spectra Physics Model 3900). The laser is pumped by the all lines output of an argon-ion laser (Spectra Physics Model 2040E) operating between 7 W and 20 W of total optical power. The position of one focusing mirror is micrometer controlled and allows for the adjustment of overall intracavity focusing without affecting cavity alignment or dispersion. This adjustment is critical since mode locking is strongly dependent upon the spatial properties of the cavity mode inside the laser rod.

The two physical processes responsible for the generation of short pulses in our cavity are self-focusing and self-phase-modulation in the laser rod. When the cavity is properly aligned, an increase in self-focusing will lead to an increase in pump overlap, and hence a higher round-trip gain for pulsed operation. This has the same effect as a fast saturable absorber.[15] In our case, the laser is aligned to produce a TEM_{02} cw profile and TEM_{00} mode-locked profile. The alignment of cavity mirrors is identical in the two cases. The pulse spectral content is further increased by self-phase-modulation in the laser rod. To the extent that this spectral content is phase-locked in a compressible manner, we expect the pulse duration to decrease as the intracavity power is increased.

Self-mode-locking is initiated by a regeneratively-driven,[16, 17] intracavity acousto-optic modulator (AOM) (Brimrose Model FSML-4.4-2-C*). A portion of the output from the laser is incident upon a photodiode. Under cw operation, axial mode beating produces a ~ 100-MHz component at the photodiode which is then filtered, divided by 2, passed through a variable phase delay, amplified, and used to drive the AOM. At 5 W of rf power, our AOM has a minimum modulation depth of 20% over a continuous range of modulation frequencies from 70 MHz to 110 MHz. This high nonresonant modulation depth not only provides the initial perturbation required for self-mode-locking to begin, but also helps to suppress concurrent cw modes that develop under highest power operation. This latter effect is confirmed by the observation that, when the AOM is turned off, one or more narrow lines appear over the otherwise unchanged pulse spectrum. By regeneratively driving the AOM, one avoids the need to accurately match the cavity length and thus round-trip time to a fixed rf frequency.

4.2. Reduction of cavity cubic phase errors

An important consideration for short pulse oscillators is the control of pulse broadening due to uncompensated dispersion in the laser cavity. To understand this distortion, consider the Taylor series expansion of pulse delay, τ, as a function of pulse the carrier frequency given in Eq. (1). We may consider any

$$\tau(\omega) = \left.\frac{d\phi}{d\omega}\right|_{\omega_0} + (\omega-\omega_0)\left.\frac{d^2\phi}{d\omega^2}\right|_{\omega_0} + \frac{1}{2}(\omega-\omega_0)^2\left.\frac{d^3\phi}{d\omega^3}\right|_{\omega_0} + \frac{1}{6}(\omega-\omega_0)^3\left.\frac{d^4\phi}{d\omega^4}\right|_{\omega_0} \cdots \qquad \text{Eq. (5)}$$

short pulse to be composed of longer duration pulses of different frequency and amplitude. An estimate of the pulse broadening on one round trip of the laser cavity may then be obtained by considering the delay of two pulses with carrier ω_0 and $\omega_0+\Delta\omega/2$. In general, an intracavity prism pair is used to compensate for the large positive group delay dispersion (GDD), $d^2\phi/d\omega^2$, of the laser material and intracavity AOM. However, for pulses shorter than ~ 50 fs, higher-order terms in the Taylor expansion become important. In particular, the cubic phase error ($d^3\phi/d\omega^3$) of the laser cavity may limit the pulse duration.[4, 18] The net dispersion of a prism pair is determined by the composition, apex angle, angle of incidence, intraprism path length, and interprism separation. We use a dispersive ray-tracing analysis to exactly calculate the effects of all of these parameters on all orders of dispersion. To minimize intracavity loss, the apex angle is chosen such that the central wavelength enters and exits the prisms at Brewster's angle. For a desired amount of negative GDD, the interprism separation is then determined by the prism composition and the intraprism path length. If we choose the prism pair GDD to exactly cancel the round-trip GDD of the other cavity elements, the net round-trip dispersive error of the cavity is dominated by the cubic phase term.

In Fig. 2, we show the round-trip, cubic phase error, at 800 nm, as a function of prism composition and single pass, intraprism path length, for a net zero GDD cavity consisting of a 2 cm sapphire rod and a prism pair. From Fig. 2, we see that the cavity cubic phase error is minimized for most of the materials shown when the beam passes as closely as possible to the

prism apices (typical cavity beams require ~ 2 mm of prism insertion). This effect is especially pronounced for high dispersion materials such as SF10. It should also be clear from Fig. 2 that minimizing intraprism path length does not always minimize cubic phase error. For BeO,[19] there is actually a finite intraprism path length that simultaneously nulls GDD and cubic phase. Unfortunately, optical quality BeO is not a commercially available material. The next best choice of material would be fused silica; however, the interprism separation required to compensate for our rod and AOM (12 mm silica) is 143 cm. This separation is too large to allow stable mode formation with the intracavity elements of our laser. We use LaK31 prisms, with the required separation being only 50 cm, yielding a residual cubic phase error that is 60% less than a cavity with SF10 prisms.

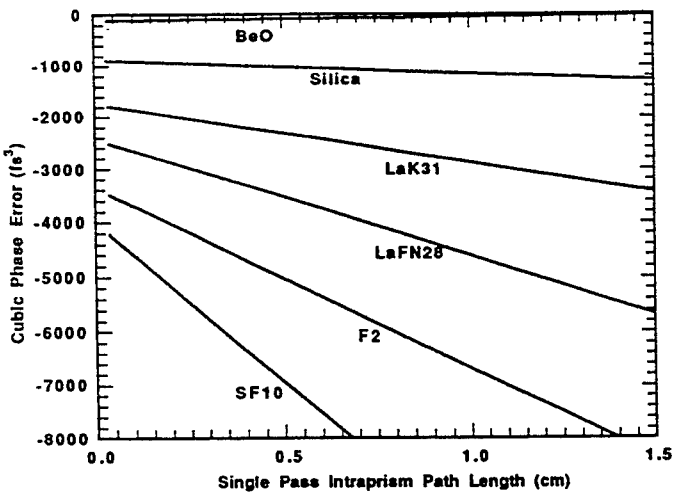

Figure 2. Cavity round-trip cubic phase for a 1-cm sapphire rod and zero net GDD.

4.3. Elimination of cavity cubic phase errors

For common prism materials and operation at 800 nm, lowering the intracavity material paths will reduce, but not eliminate, cavity cubic phase errors. However, at wavelengths longer than 800 nm, the magnitude of the negative cubic phase contribution of prism pairs decreases relative to sapphire. It thus becomes possible at certain wavelengths for situations similar to that depicted for BeO in Fig. 2 to occur for common materials.[20] The often-made assumption that cavity cubic phase is minimized when intraprism material is minimized is incorrect for prisms made of these materials at these wavelengths. At these wavelengths cavity cubic phase may be eliminated for finite prism insertion. The range over which phase may be eliminated in Ti:sapphire cavities varies from ~ 850 nm for silica all the way to ~ 1040 nm for SF10. It should be noted that sub-100-fs pulse generation in Ti:sapphire has been demonstrated throughout this wavelength range, with pulses as short as 62 fs having been reported as far in the infrared as 1053 nm.[21]

4.4. Increase of pulse spectral content

While the reduction of intracavity phase errors will allow shorter pulses to propagate without distortion, the duration of the pulse will be determined by its spectral content. This content may be increased by increasing the amount of self-phase-modulation that occurs in the laser rod, which, in turn, is accomplished by increasing the intracavity pulse energy. Increasing the intracavity pulse energy may be accomplished by decreasing the cavity output coupling, or more easily by raising the pump power. Raising the pump power, however, changes the amount of thermal lensing and, to a lesser extent, self focusing, that occurs in the laser rod. This change can be compensated for without affecting intracavity alignment or dispersion by adjusting a translatable intracavity focusing mirror. In this way, we can reproduce the far-field cw profile over a wide range of pump powers (between 7 W and 20 W). Mode locking then immediately ensues when the AOM is turned on. Figure 3 shows the increase of pulse spectral content and the corresponding decrease in pulse duration as the intracavity power is increased. The focusing mirror was translated 230 μm over the full range shown. The spectral structure which develops at higher powers is indicative of self-phase-modulation. It should be noted that, at the highest powers, the high-modulation-depth AOM not only initiates self-mode-locking but also inhibits any concurrent cw mode operation.

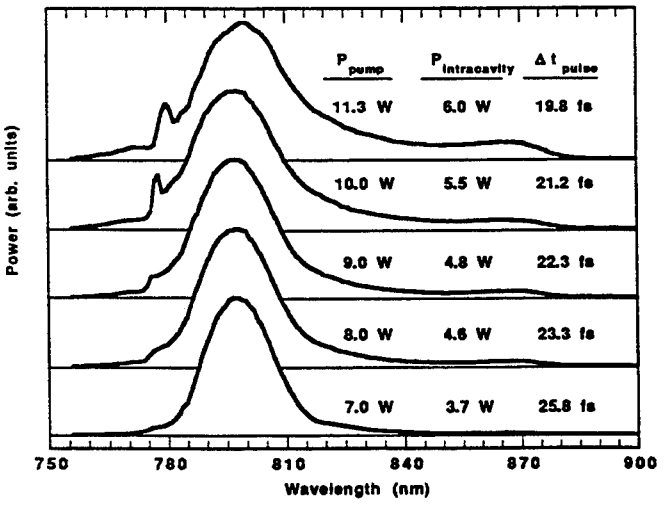

Figure 3. Pulse spectrum and pulse duration at five intracavity powers. The output coupling in 10%.

4.5. Bifurcation and double pulsing

Figure 3 suggests that we might further reduce the pulse duration by increasing the intracavity power beyond 6 W. However, at higher intracavity powers, the pulse bifurcates and two similar, slightly longer duration, lower energy pulses develop with a temporal separation that yields equal gain. With the AOM off, the two pulses separate by one-half the round-trip time of the cavity. With the AOM on, this separation shortens to between 10 ps and 50 ps. The exact separation is stable but is dependent upon the phase and power of the rf driving the AOM. Such closely spaced double pulses cannot be resolved with common photodiodes. The separation is also too large to be seen in typical high-resolution autocorrelations. To observe these pulses, the output of the laser was monitored with a 2-ps resolution streak camera (Hamamatsu Model c1587). A typical streak trace is shown in Fig. 4. Although a quantitative study has not been conducted, it is believed that this mode of operation should provide a convenient method for producing electronically controllable, variable delay, collinear pulses. Autocorrelations of the individual pulses indicate a duration of ~ 22 fs with a total output power of ~ 2 W.

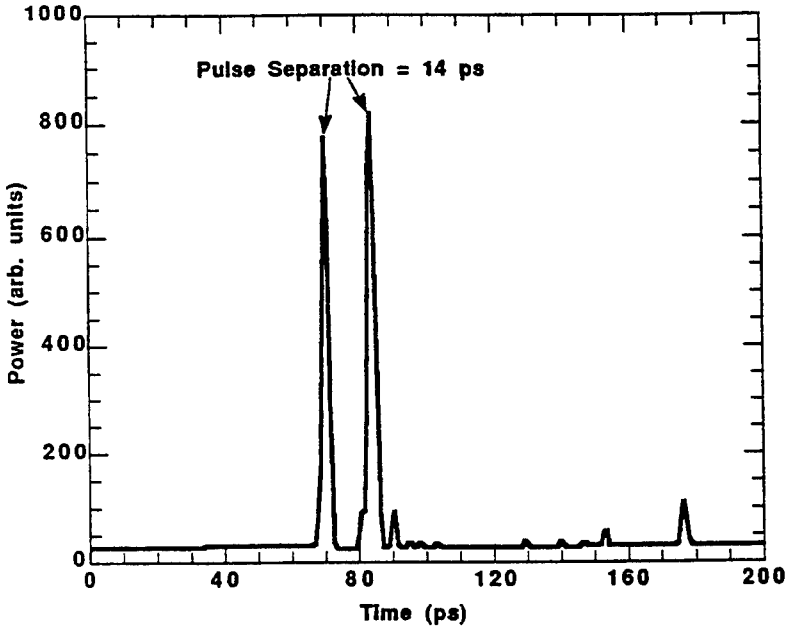

Figure 4. Streak camera trace of double pulse operation.

Bifurcation limits the intracavity power and hence the peak power of the output pulses. However, by scaling to larger output coupling, one may obtain a higher output at the same intracavity power. Simple scaling implies that, if one increases the output coupling from 10% to 15%, the pump power should be increased from 11.3 W to ~ 16 W in order to produce the same intracavity pulse energy. Under these conditions, we observe 22-fs pulses with a peak power of 430 kW. At a slightly higher pump power (19 W) we have obtained 21-fs, ~ 500 kW peak power pulses with an average output power of 1.05 W. Uncompensatable thermal focusing limits the output power in the latter case.

5. Amplification Considerations

5.1. Chirped pulse amplification

Although many amplification systems now exist that are capable of producing terawatt (~ 100-fs) pulses, the amplification of 20-fs pulses to similar levels will require significant design changes. These changes are necessary to avoid a variety of linear and nonlinear pulse distortions which manifest themselves at short pulse durations. In particular, amplification systems based on chirped pulse amplification (CPA) will require new expander/compressor designs, elimination of refractive optics, and enclosure of compression stages in vacuum.

5.2. Quintic phase-limited 10,000 times expansion/compression

The key to all chirped pulse amplification systems is the ability to expand a seed pulse in time, amplify this long pulse, and then recompress the amplified pulse to the original pulse duration. Traditional pulse expanders, based on a pair of antiparallel gratings and a one-to-one refractive telescope,[22] can produce pulse distortions due to frequency-dependent material paths through the system. To avoid this problem, we have designed and constructed a cylindrical mirror-based pulse expander. In order to calculate the dispersive characteristics of this expander, including material in the amplification chain and the pulse compressor, we use a dispersive ray-tracing analysis. This analysis includes the effects of finite beam size and divergence, both of which are significant on a 20-fs time scale. The beam traverses the system twice. On the first pass, a finite size beam experiences a spatially varying pulse expansion due to the mirror/grating asymmetry of our "z-fold" arrangement. This unwanted distortion, which can be greater than the pulse duration, may be removed by inverting the beam in the horizontal plane before a second pass through the system. The result is a spatially uniform, expanded beam, which may be amplified and recompressed. The degree to which one may recompress to the original pulse duration is dependent upon cancellation of frequency-dependent phase shifts in the expander, amplifier, and compressor. We show numerically that it is possible, with the correct choice of compressor grating angle and separation and correct amount of material path, to cancel cubic and quartic phase distortion. Calculations indicate that it

should be possible to expand 20-fs pulses by > 10,000 times and recompress to within 1-fs of the original pulse duration, the final error being quintic phase limited.

5.3. Errors due to refractive optics

It is known that refractive optics, especially singlets, may lead to uncompensatable pulse distortions when used with ultrashort pulses.[23] This effect arises from the fact that different parallel input rays traverse different material paths in an optical system. This fact manifests itself in two ways. First, it leads to a delay of the chief ray with respect to the marginal ray, i.e., a curved pulse front; second, it leads to a spatially varying pulse broadening. Both of these effects cannot be compensated for in a convenient manner. In order to calculate possible distortions due to amplifier beam expansion telescopes, we use a dispersive ray-tracing analysis. The results of one such calculation are depicted in Fig. 5. In this plot, we present pulse delay as a function of input beam diameter for a 6.7-times magnification, Galilean telescope based on BK7 glass lenses. Also included in this plot is a paraxial analysis of the same telescope using the formulas of Bor.[23] As can be seen, the distortion for reasonable input beam diameters is on the order of our 20-fs pulse. This distortion leads to a longer effective pulse duration. It can also be seen from the figure that the ray-tracing analysis predicts larger pulse front curvatures. This increased distortion is a result of spherical aberration. The effect of spatially-varying dispersive broadening is less significant. In order to avoid both effects we have constructed reflective telescopes based on cylindrical optics. Due to the relatively large diameter of the input beams to these telescopes, each dimension may be expanded sequentially without introduction of significant astigmatism.

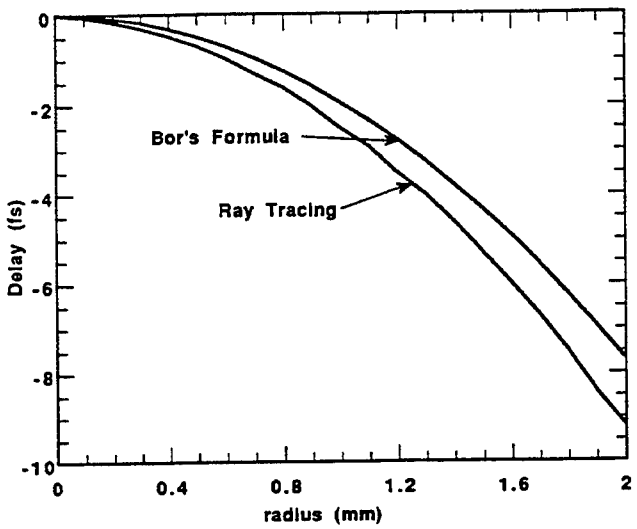

Figure 5. Pulse delay vs. beam radius, 6.7-X magnification.

5.4. Nonlinear distortion after compression

The current amplifier design should allow the production of 5-TW pulses (125 mJ in 25 fs) at a 10-Hz repetition rate. In this design, the final beam diameter will be 23 mm. This implies an unfocused intensity of 1.2×10^{12} W/cm^2 after pulse compression. At these intensities, self-phase-modulation in air (nonlinear index = 6.3×10^{-19} cm^2/W) is sufficient to cause a pi phase shift in ~ 0.5 m. Self-phase-modulation in vacuum window materials would also be of the same magnitude. In order to avoid these distortions, it is necessary to place the compression stage and experiments in vacuum chambers.

6. Conclusions

The oscillator and amplifier described here should allow a higher x-ray yield per laser pulse, or equivalent yield to previous experiments, with less laser energy. The x-ray pulses generated will be used to test the feasibility of time-gated detection in medical imaging applications. The high peak power laser pulses will also be used in x-ray laser experiments.

7. Acknowledgements

The work described here was supported by the Air Force Office of Scientific Research, the Army Research Office, the Strategic Defense Initiative Organization, the Office of Naval Research and through generous equipment loans from the Lawrence Livermore National Laboratory. B. E. Lemoff acknowledges the support of a National Science Foundation Graduate Fellowship.

8. References

1. B. E. Lemoff and C. P. J. Barty, Opt. Lett., **17**, 19, 1367-1369, 1992.
2. C.-P. Huang, M. T. Asaki, S. Backus, M. M. Murnane, H. C. Kapteyn and H. Nathel, Opt. Lett., **17**, 18, 1289-1291, 1992.
3. B. Proctor and F. Wise, Opt. Lett., **17**, 18, 1295-1297, 1992.

4. F. Krausz, M. E. Fermann, T. Brabec, P. F. Curley, M. Hofer, M. H. Ober, C. Spielmann, E. Wintner and A. J. Schmidt, IEEE J. Quantum Electron., **QE-28**, 10, 2097-2122, 1992.
5. J. D. Kmetec, J. J. Macklin and J. F. Young, Opt. Lett., **16**, 13, 1001-1003, 1991.
6. A. Sullivan, H. Hamster, H. C. Kapteyn, S. Gordon, W. White, H. Nathel, R. J. Blair and R. W. Falcone, Opt. Lett., **16**, 18, 1406-1408, 1991.
7. J. D. Kmetec, C. L. Gordon III, J. J. Macklin, B. E. Lemoff, G. S. Brown and S. E. Harris, Phys. Rev. Lett., **68**, 10, 1527-1530, 1992.
8. J. D. Kmetec, IEEE J. Quantum Electron., **QE-28**, 10, 2382-2387, 1992.
9. A. H. Compton and S. K. Allison, X-Rays in Theory and Experiment, Van Nostrand, New York, 1935.
10. F. Salin, J. Squier, G. Mourou and G. Vaillancourt, Opt. Lett., **16**, 24, 1964-1966, 1991.
11. A. Macovski, Medical Imaging Systems, Prentice-Hall, Inc., Englewood, NJ, 1983.
12. K. Koehler, CATH Lab, Stanford University Medical Center, Stanford, CA, personal communication.
13. J. D. Kilkenny, P. Bell, G. Hanks, G. Power, R. E. Turner and J. Wiedwald, Rev. Sci. Instrum., **59**, 8, 1793-1796, 1988.
14. G. S. Brown, Stanford Linear Accelerator Center, Stanford, CA, personal communication.
15. D. E. Spence, P. N. Kean and W. Sibbett, Opt. Lett., **16**, 1, 42-44, 1991.
16. D. E. Spence, J. M. Evans, W. E. Sleat and W. Sibbett, Opt. Lett., **16**, 22, 1762-1764, 1991.
17. J. D. Kafka, M. L. Watts and T. Baer, Digest of Conference on Lasers and Electro-Optics, Paper JMB3, Optical Society of America, Washington, D. C., 1991.
18. H. A. Haus, J. D. Moores and L. E. Nelson, Opt. Lett., **18**, 1, 51-53, 1993.
19. M. J. Weber, ed., CRC Handbook of Laser Science and Technology, Vol. 3, p. 193, CRC Press, Boca Raton, FL, 1986.
20. B. E. Lemoff and C. P. J. Barty, Opt. Lett., **18**, 1, 57-59, 1993.
21. J. D. Kafka, M. L. Watts and J.-W. J. Pieterse, IEEE J. Quantum Electron., **QE-28**, 10, 2151-2162, 1992.
22. O. E. Martinez, IEEE J. Quantum Electron., **QE-23**, 1, 59-64, 1987.
23. Z. Bor, J. Mod. Opt., **35**, 12, 1907-1918, 1988.